

Crystal structures, electronic properties and structural pathways of two $[\text{Cu}(\text{phen})_2(\text{OH}_2)][\text{Y}]_2$ complexes (phen = 1,10-phenanthroline, $\text{Y} = \text{CF}_3\text{SO}_3^-$ or ClO_4^-)[†]

Gillian Murphy, Clair Murphy, Brian Murphy and Brian Hathaway*

The Chemistry Department, University College Cork, Ireland

The crystal structures of $[\text{Cu}(\text{phen})_2(\text{OH}_2)][\text{CF}_3\text{SO}_3]_2$ **1** and $[\text{Cu}(\text{phen})_2(\text{OH}_2)][\text{ClO}_4]_2$ **2** (phen = 1,10-phenanthroline) have been determined by diffractometer data collection. The CuN_4O chromophores in both complexes **1** and **2** lie on a crystallographic two-fold axis, with a square pyramidal distorted trigonal bipyramidal stereochemistry, an elongation along the Cu–O direction, Cu–O 2.066(3) and 2.245(4) Å, and an increase in the N(4)–Cu–N(2) α_3 angle to 123.4(1) and 136.0(1)°, respectively. This suggests that the stereochemistry of **1** is best described as near regular trigonal bipyramidal, RTB, and that of **2** as square based pyramidal distorted trigonal bipyramidal, SBPDTB. The structures of **1** and **2** were compared by scatter-plot analysis, with other $[\text{Cu}(\text{chelate ligand})_2(\text{OH}_2)][\text{Y}]_2$ complexes involving two-fold axes of symmetry. This shows that the spread of the data points is not random, is relatively large and suggests the presence of vibronic coupling to account for the distortion from the RTB CuN_4O chromophore, along the C_2 dominated +A and –A route distortions. A continuous linear structural pathway is suggested, determined by the coupled $\nu_{\text{sym}}^{\text{str}}$ and $\nu_{\text{sym}}^{\text{bend}}$ modes of vibration, involving a progression of 40–50 modes, spanning an angular distortion range of 91–140°, which correlate with electronic and ESR spectral data.

The concept of a structural pathway,^{2,3} Fig. 1, for $[\text{Cu}(\text{chelate ligand})_2\text{X}][\text{Y}]$ type complexes has recently been developed for nine complexes of the $[\text{Cu}(\text{bipy})_2\text{Cl}]^+$ cation^{4,5} (bipy = 2,2'-bipyridyl) using scatter plots⁶ and factor analysis.^{7,8} The effect of changing the co-ordinated anion, X, from Cl^- to Br^- and I^- has emphasised both similarities and differences.⁵ It is now realised that the original treatment⁵ of the nine $[\text{Cu}(\text{bipy})_2\text{Cl}][\text{Y}]$ complexes together was hardly justified,⁹ and that they are better treated as a group of six ($\tau = 0.6$ –0.8) and a group of three ($\tau \approx 1.0$), where $\tau = (\alpha_8 - \alpha_1)/60$.¹⁰ The former show a –A + B type distortion, Fig. 1,⁹ with α_3 values clearly <120°, 96.5–115.5°, due to –A route distortion, and α_1 values >120°, with α_2 values <120°, suggesting +B route distortion. The remaining three complexes have α_3 values slightly greater than 120°, in the range 122.6–123.8°. This suggests that small +A route distortions are operating, Fig. 1, involving the alternative mode of distortion of the regular trigonal bipyramidal (RTB) CuN_4X chromophore, towards a regular square based pyramid (RSBP), with elongation along the Cu–X direction and α_3 slightly greater than 120°. This paper examines the $\pm A$ route distortions of $[\text{Cu}(\text{chelate ligand})_2\text{X}][\text{Y}]$ complexes and reports the preparation and crystal structure determinations of two $[\text{Cu}(\text{phen})_2(\text{OH}_2)][\text{Y}]_2$ complexes, where phen = 1,10-phenanthroline and $\text{Y} = \text{CF}_3\text{SO}_3^-$ **1** or ClO_4^- **2**, respectively. The structure of **2** has been previously reported¹¹ in an incorrect space group, $P\bar{1}$, with the CuN_4O chromophore in a general position. The structures of the complexes where $\text{Y} = \text{BF}_4^-$ **3**¹² or NO_3^- **4**¹³ have been determined previously, and are compared with those of **1** and **2** by scatter-plot analysis.

Experimental

Preparations

The complex $[\text{Cu}(\text{phen})_2(\text{OH}_2)][\text{CF}_3\text{SO}_3]_2$ **1** was prepared by adding a hot solution of phen (0.36 g, 2 mmol) in propanone (150 cm³) to a hot aqueous solution (30 cm³) of $\text{Cu}(\text{CF}_3\text{SO}_3)_2$ (0.36 g, 1 mmol). The resulting solution yielded emerald-green needles of **1** after 3 d (Found: C, 42.25; H, 2.45; Cu, 8.2; N, 7.4. $\text{C}_{26}\text{H}_{18}\text{CuF}_6\text{N}_4\text{O}_7\text{S}_2$ requires C, 42.2; H, 2.45; Cu, 8.6; N, 7.55%).

The complex $[\text{Cu}(\text{phen})_2(\text{OH}_2)][\text{ClO}_4]_2$ **2** was prepared by adding phen (0.36 g, 2 mmol) to a hot solution (EtOH–water, 1:1, 100 cm³) of $[\text{Cu}(\text{OH}_2)_6][\text{ClO}_4]_2$ (0.37 g, 1 mmol). The solution was boiled and the immediate turquoise precipitate filtered off. The resulting hot solution yielded green crystals of **2** overnight (Found: C, 44.8; H, 2.95; Cu, 9.75; N, 8.75. $\text{C}_{24}\text{H}_{18}\text{Cl}_2\text{CuN}_4\text{O}_9$ requires C, 44.95; H, 2.8; Cu, 9.4; N, 8.75%).

CAUTION: perchlorates are explosive!

Crystallography

The crystal and refinement data for complexes **1** and **2** are shown in Table 1. The unit-cell dimensions were determined from 25 reflections (θ 3–25°) and the intensities collected on an Enraf-Nonius CAD4 X-ray diffractometer with graphite-monochromatised Mo-K α radiation (λ 0.710 69 Å). Reflections in the range $3.0 < \theta < 24^\circ$ in one quadrant were collected at room temperature using an ω –2 θ scan. A constant scan speed of 7° min^{-1} was used, with a variable scan width ($0.8 + 0.2 \tan \theta$). With an acceptance criterion $I > 2.5\sigma(I)$, 2219 and 1826 reflections were retained for **1** and **2**, respectively. Lorentz-polarisation corrections were applied, but no correction was made for absorption. Data reduction was carried out using the program XCAD.¹⁴ The structures were solved using the SHELX 76¹⁵ and SHELXS 86¹⁶ programs, by Patterson and direct methods procedures, developed by Fourier difference techniques and refined by least-squares analysis, $\sum w(|F_o| - |F_c|)^2$, with the initial $w = 1/[\sigma^2(F_o)]$ and final $w = k/[\sigma^2(F_o) + g(F_o)^2]^{-1}$. Anisotropic thermal parameters were used for all the non-hydrogen atoms. The positions of the hydrogen atoms were calculated and 'floated' on the associated carbon and oxygen atom positions. Complex atom scattering factors were employed.¹⁷ All calculations were carried out using the SHELX 76,¹⁵ SHELXS 86,¹⁶ XANADU,¹⁸ PUBTAB,¹⁹ and XCAD¹⁴ programs on the University College Cork (U.C.C.) mainframe

[†] Comparative crystallography. Part 4.¹

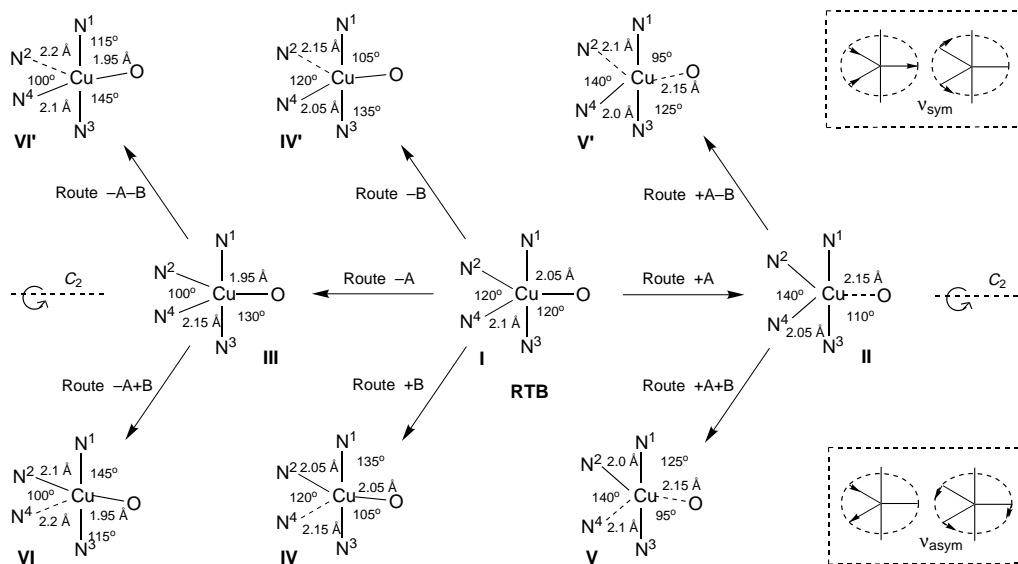


Fig. 1 The forms of distortion of the RTB CuN_4O chromophore involving the $\pm A$, $\pm B$ and $\pm A \pm B$ routes (bond distances are quoted to the nearest 0.05 Å)

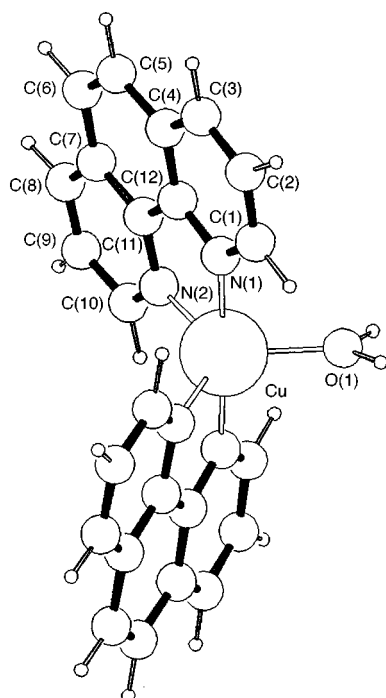


Fig. 2 Molecular structure of the $[\text{Cu}(\text{phen})_2(\text{OH}_2)]^{2+}$ cation of complex **1**

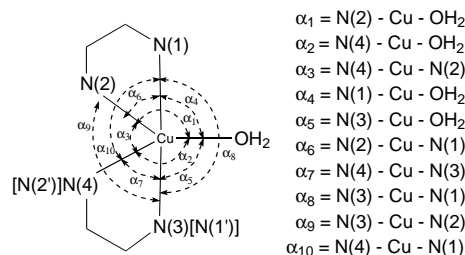


Fig. 3 The atom numbering scheme and α_n notation for the CuN_4O chromophore. In order to retain compatibility with the non-two-fold chromophores, the notation N(3) [N(1')] and N(4) [N(2')] is used

Results and Discussion

Crystal structures

The structure of complex **1** consists of a $[\text{Cu}(\text{phen})_2(\text{OH}_2)]^{2+}$ cation and two $[\text{CF}_3\text{SO}_3]^-$ anions per asymmetric unit. Each phen is involved as a bidentate chelate ligand, co-ordinating to the copper through the nitrogen atoms, with the oxygen atom of the water ligand occupying the fifth co-ordination site. The copper and oxygen atoms of the chromophore lie on a crystallographic two-fold axis. The $[\text{Cu}(\text{phen})_2(\text{OH}_2)]^{2+}$ cation has a five-co-ordinate CuN_4O chromophore, with a slightly distorted trigonal bipyramidal stereochemistry. The out-of-plane bond distances, $\text{Cu}-\text{N}(1,3)$ 1.994(3) Å, Table 2, are significantly shorter than the in-plane distances, $\text{Cu}-\text{N}(2,4)$ 2.084(2) Å, $\Delta N_{1,2} = 0.090$ Å, a difference of *ca.* 0.1 Å as previously observed.²¹ The oxygen atom co-ordinates in the plane at a $\text{Cu}-\text{O}$ distance of 2.066(3) Å. The α_8 angle of $177.0(1)^\circ$ is almost linear. The out-of-plane bond angles, $\alpha_4 = \alpha_5 = 91.5(1)^\circ$, are slightly greater than 90° , resulting in both the N(1) and N(3) atoms bending away from the $\text{Cu}-\text{O}$ bond, indicating the presence of a trigonal rather than a tetrahedral distortion of the CuN_4 chromophore.^{22,23} The in-plane angles distort slightly from the 120° of a RTB stereochemistry, with $\alpha_1 = \alpha_2 = 118.3(1)^\circ$ and $\alpha_3 = 123.4(1)^\circ$. These distortions suggest that the stereochemistry is best described as a near regular trigonal bipyramidal CuN_4O chromophore (RTB), with a slight elongation along the $\text{Cu}-\text{O}$ distance, namely the +A route of distortion, Fig. 1. The $[\text{CF}_3\text{SO}_3]^-$ anion was refined as a disordered group, since its anisotropic thermal parameters were high, with the linked pairs of F(1)/F(1'), F(2)/F(2'), F(3)/F(3'), O(2)/O(2'), O(3)/O(3') and O(4)/O(4') all having site occupation

VAX 6310 computer; PLUTON 92²⁰ was run on a Memorex 386 personal computer.

Selected bond lengths and angles are given in Table 2. Fig. 2 shows the molecular structure of the $[\text{Cu}(\text{phen})_2(\text{OH}_2)]^{2+}$ cation of **1**, and Fig. 3 the atom numbering scheme involved and the α_n bond angle notation used.

Atomic coordinates, thermal parameters, and bond lengths and angles have been deposited at the Cambridge Crystallographic Data Centre (CCDC). See Instructions for Authors, *J. Chem. Soc., Dalton Trans.*, 1997, Issue 1. Any request to the CCDC for this material should quote the full literature citation and the reference number 186/552.

The diffuse reflectance spectra were recorded as polycrystalline samples on a Shimadzu UV-VIS 3101 PC spectrometer, over the range 5000–30 000 cm^{-1} .

Table 1 Crystallographic and structure refinement data* for [Cu(phen)₂(OH₂)][CF₃SO₃]₂ **1** and [Cu(phen)₂(OH₂)][ClO₄]₂ **2**

	1	2
Formula	C ₂₆ H ₁₈ CuF ₆ N ₄ O ₇ S ₂	C ₂₄ H ₁₈ Cl ₂ CuN ₄ O ₉
<i>M</i>	740.1	640.9
<i>a</i> /Å	25.833(4)	19.078(2)
<i>b</i> /Å	10.024(3)	8.173(3)
<i>c</i> /Å	16.321(3)	16.239(2)
β/°	136.16(1)	100.14(2)
<i>U</i> /Å ³	2927.29	2492.82
<i>D_c</i> /g cm ^{−3}	1.68	1.71
<i>F</i> (000)	1492	1299
μ/cm ^{−1}	9.24	10.97
No. unique reflections (<i>N</i>)	2219	1826
No. varied parameters (<i>P</i>)	264	201
<i>N/P</i>	8.41	9.09
<i>R</i>	0.0620	0.0749
<i>R'</i>	0.0604	0.0741
<i>k</i>	1.0000	1.000
<i>g</i>	0.038 16	0.040 33
Maximum final shift/e.s.d.	0.002 (cation)	0.001
Residual electron density/e Å ^{−3}	0.050 (CF ₃ SO ₃ [−] anion)	0.001
No. atoms with anisotropic thermal parameters	+0.41, −0.90 30	+0.56, −0.96 23

* Details in common = monoclinic, space group *C2/c* (*C*_{2h} no. 15); *Z* = 4.

Table 2 Selected bond lengths (Å) and angles (°) for the [Cu(chelate ligand)₂(OH₂)]₂[Y]₂ and [Cu(phen)₂X][Y] complexes

Chelate X Y	phen OH ₂ CF ₃ SO ₃ 1	phen OH ₂ ClO ₄ 2	phen OH ₂ BF ₄ 3 ¹²	phen OH ₂ NO ₃ 4 ¹³	bipy OH ₂ $\frac{1}{2}$ (S ₂ O ₆) 5 ²⁴	bipym OH ₂ ClO ₄ ·H ₂ O 6 ²⁵	bipym OH ₂ PF ₆ ·H ₂ O 7 ²⁶	bipy OH ₂ $\frac{1}{2}$ (S ₂ O ₆) 8 ²⁷	phen Br ClO ₄ 9 ²⁹	phen I PF ₆ 10 ³⁰	phen I I.S ₃ 11 ³¹
Cu–O(X)*	2.066(3)	2.245(4)	2.238(8)	2.180(3)	2.158(15)	1.993(4)	1.982(5)	2.054(5)	2.066(1)	2.052(2)	2.079(3)
Cu–N(1)	1.994(3)	1.980(4)	1.985(6)	1.989(3)	1.977(9)	1.993(4)	1.994(3)	1.973(6)	1.985(5)	1.988(7)	2.000(10)
Cu–N(2)	2.084(2)	2.032(3)	2.041(7)	2.028(2)	2.013(9)	2.094(4)	2.080(3)	2.024(6)	2.091(3)	2.086(7)	2.100(10)
Cu–N(3)	1.994(3)	1.980(4)	1.985(6)	1.989(3)	1.977(9)	1.993(4)	1.994(3)	1.983(5)	1.985(5)	1.988(7)	2.000(10)
Cu–N(4)	2.084(2)	2.032(3)	2.041(7)	2.028(2)	2.013(9)	2.094(4)	2.080(3)	2.123(6)	2.091(3)	2.086(7)	2.100(10)
α ₁	118.3(1)	112.0(1)	111.7(3)	110.2(1)	115.1(3)	130.1(1)	128.6(1)	143.6(1)	119.8(1)	122.3(2)	125.3(3)
α ₂	118.3(1)	112.0(1)	111.7(3)	110.2(1)	115.1(3)	130.1(1)	128.6(1)	104.9(2)	119.8(1)	122.3(2)	125.3(3)
α ₃	123.4(1)	136.0(1)	136.6(3)	139.6(1)	129.8(3)	99.8(1)	102.8(1)	111.4(3)	120.6(2)	115.4(2)	109.4(3)
α ₄	91.5(1)	86.9(1)	86.4(3)	85.8(1)	87.3(3)	90.5(1)	90.8(1)	89.0(2)	91.5(1)	91.5(2)	92.3(3)
α ₅	91.5(1)	86.9(1)	86.4(3)	85.8(1)	87.3(3)	90.5(1)	90.8(1)	91.4(2)	91.5(1)	91.5(2)	92.3(3)
α ₆	81.5(1)	82.2(1)	82.6(3)	82.9(1)	81.4(4)	79.8(1)	80.1(1)	81.2(3)	81.1(2)	81.9(3)	80.4(4)
α ₇	81.5(1)	82.2(1)	82.6(3)	82.9(1)	81.4(4)	79.8(1)	80.1(1)	79.3(2)	81.1(2)	81.9(3)	80.4(4)
α ₈	177.0(1)	173.8(1)	172.8(3)	171.6(1)	174.6(3)	179.0(1)	178.3(1)	179.1(2)	177.0(2)	176.9(3)	175.5(4)
α ₉	97.1(1)	100.2(1)	100.1(3)	100.0(1)	100.9(3)	99.5(1)	98.8(1)	98.0(2)	97.5(2)	96.5(2)	97.0(4)
α ₁₀	97.1(1)	100.2(1)	100.1(3)	100.0(1)	100.9(3)	99.5(1)	98.8(1)	101.4(3)	97.5(2)	96.5(2)	97.0(4)
τ _A	0.89	0.63	0.60	0.53	0.75	1.32	1.26	1.13	0.95	1.03	1.10

* The Cu–X distances have been corrected to Cu–O(X) distances^{6,7} using the relationships: Cu–Br −0.43 Å and Cu–I −0.62 Å.

factors (s.o.f.s) of 0.5. This procedure resulted in lower anisotropic thermal parameters for the [CF₃SO₃][−] anion.

The asymmetric unit of complex **2** consists of a [Cu(phen)₂(OH₂)]²⁺ cation and two [ClO₄][−] anions. The copper and oxygen atoms of the CuN₄O chromophore lie on a crystallographic two-fold axis. The axial and equatorial Cu–N distances, Table 2, are significantly different at 1.980(4) and 2.032(3) Å, respectively, Δ*N*_{1,2} = 0.052 Å, less than the 0.1 Å normally observed.²¹ The oxygen atom co-ordinates in the plane at a Cu–O distance of 2.245(4) Å. The α₈ angle of 173.8(1)° is less than the expected value of 180°. The out-of-plane bond angles, α₄ = α₅ = 86.9(1)°, are less than 90°, resulting in both the N(1) and N(3) atoms bending towards the Cu–O bond and indicating a tetrahedral distortion of the CuN₄ chromophore. The α_{1,2} angles are less than 120°, 112.0(1)°, while the α₃ angle is greater than 120°, at 136.0(1)°. Together this suggests that the stereochemistry of **2** is best described as a square based pyramidal distorted trigonal bipyramidal (SBPDTB) CuN₄O chromophore, with a significant elongation along the Cu–O direction, namely the +A route of the structural pathway of Fig. 1. The [ClO₄][−] anion was refined as a disordered group since the anisotropic

thermal parameters were high. Two additional oxygen atoms, O(6) and O(7), were added to O(4) and O(5), each having a s.o.f. of 0.5; this disorder probably accounts for the high *R* value of **2**.

Comparison of complexes **1** and **2** with [Cu(phen)₂(OH₂)]₂[Y]₂ complexes of known structure

There are two other [Cu(phen)₂(OH₂)]₂[Y]₂ complexes of known crystal structure, Y = BF₄[−] **3**¹² or NO₃[−] **4**¹³. All four [Cu(phen)₂(OH₂)]₂[Y]₂ complexes have five-co-ordinate CuN₄O chromophores, with the copper and oxygen atoms lying on a crystallographic two-fold axis. Table 2 lists selected bond lengths, angles and τ_A values of the four [Cu(phen)₂(OH₂)]₂[Y]₂ complexes, where τ_A = (α₈ − α₃)/60,⁹ in which the α₃ angle is used to distinguish the elongation along the Cu–O rather than the Cu–N(4) direction. The stereochemistries of the five-co-ordinate CuN₄O chromophores, Table 2, vary from near RTB to SBPDTB, which is reflected in a range of τ_A values from 0.89 to 0.53, Δτ_A = 0.36. Complex **1** has a near RTB stereochemistry, τ_A = 0.89, while **2–4** have τ_A values in the more limited range of

Table 3 Sums of the in-plane bond angles and distances for the $[\text{Cu}(\text{chelate ligand})_2(\text{OH}_2)][\text{Y}]_2$ complexes

	Complex						
	1	2	3	4	5	6	7
$\alpha_1/^\circ$	118.3	112.0	111.7	110.2	115.1	130.1	128.6
$\alpha_2/^\circ$	118.3	112.0	111.7	110.2	115.1	130.1	128.6
$\alpha_3/^\circ$	123.4	136.0	136.6	139.6	129.8	99.8	102.8
Sum/ $^\circ$	360.0	360.0	360.0	360.0	360.0	360.0	360.0
Cu–O/ \AA	2.066	2.245	2.238	2.180	2.158	1.993	1.982
Cu–N(2)/ \AA	2.084	2.032	2.041	2.028	2.013	2.094	2.080
Cu–N(4)/ \AA	2.084	2.032	2.041	2.028	2.013	2.094	2.080
Sum/ \AA	6.234	6.309	6.320	6.236	6.184	6.181	6.142

Table 4 Suggested RTB and extreme $\pm A$ stereochemistries for the CuN_4O chromophore

	RTB	+A (RSBP)	–A (seesaw)
$\alpha_1/^\circ$	120	97.5	135
$\alpha_2/^\circ$	120	97.5	135
$\alpha_3/^\circ$	120	165	90
Cu–N(4)/ \AA	2.092	1.998	2.155
Cu–N(2)/ \AA	2.092	1.998	2.155
Cu–O/ \AA	2.064	2.253	1.938

0.63 to 0.53 and their stereochemistries are best described as SBPDTB. These four complexes with α_3 angles $>120^\circ$, $\alpha_{1,2}$ angles $<120^\circ$, increasing Cu–O distances and decreasing Cu–N(2,4) distances, plus a crystallographic two-fold axis, undergo a pure +A route distortion, Fig. 1.

Comparison of the $[\text{Cu}(\text{phen})_2(\text{OH}_2)][\text{Y}]_2$ complexes with other known $[\text{Cu}(\text{chelate ligand})_2(\text{OH}_2)][\text{Y}]_2$ complexes

There are three related $[\text{Cu}(\text{chelate ligand})_2(\text{OH}_2)][\text{Y}]_2$ complexes, which have a CuN_4O chromophore and with the copper and oxygen atoms lying on a crystallographic two-fold axis, Table 2. The $[\text{Cu}(\text{bipy})_2(\text{OH}_2)][\text{S}_2\text{O}_6]$ complex **5**²⁴ shows +A route distortion, but $[\text{Cu}(\text{bipym})_2(\text{OH}_2)][\text{ClO}_4]_2 \cdot 2\text{H}_2\text{O}$ **6**²⁵ and $[\text{Cu}(\text{bipym})_2(\text{OH}_2)][\text{PF}_6]_2 \cdot 2\text{H}_2\text{O}$ **7**²⁶ (bipym = 2,2'-bipyrimidine) show pure –A route distortion. The complex $[\text{Cu}(\text{bipy})_2(\text{OH}_2)]_2[\text{S}_5\text{O}_{10}]$ **8**²⁷ is the only known $[\text{Cu}(\text{chelate ligand})_2(\text{OH}_2)][\text{Y}]_2$ complex without a crystallographic two-fold axis and showing –A + B route distortion.

The factors limiting the angular distortion from RTB for the $[\text{Cu}(\text{phen})_2(\text{OH}_2)][\text{Y}]_2$ complexes are that the α_1 , α_2 and α_3 angles generally have values >90 or $<180^\circ$ and the sum of the angles $\alpha_1 + \alpha_2 + \alpha_3$ must add up to 360° , Table 3. A constant value for the sum of the lengths might also be expected. From Table 3 it can be seen that the latter values vary over an appreciable range, 6.234–6.320 \AA , $\Delta = 0.086$ \AA , and they differ significantly from the RTB sum of 6.248 \AA . A significant non-linear variation with τ_A occurs for the Cu–O distances, with the values for **2** and **3** larger than the predicted value by ≈ 0.1 \AA . The Cu–N(2,4) distances are constrained by the bite of the chelate ligand, whereas the Cu–O distance has no such constraint, which could explain why the in-plane distances do not have exactly constant sum values.

Scatter-plot analysis of the $\pm A$ distorted $[\text{Cu}(\text{chelate ligand})_2(\text{OH}_2)][\text{Y}]_2$ complexes

This section presents the data for the seven $[\text{Cu}(\text{chelate ligand})_2(\text{OH}_2)][\text{Y}]_2$ complexes, which have a crystallographic two-fold axis, Table 2, using scatter-plot analysis, Fig. 4(a)–4(c). The scatter plots discussed are as follows: (a) τ_A versus Cu–O, (b) Cu–O versus Cu–N(2,4) and (c) α_3 versus Cu–O. Table 4 indicates the suggested parameters for the RTB, +A (RSBP) and an extreme –A ('seesaw') stereochemistries.¹

The seven data points in Fig. 4(a) show the τ_A values decreasing from 1.32 to 0.53 as the Cu–O distances increase from 1.982(5) to 2.245(4) \AA ; τ_A values of <1.0 represent a +A route distortion, those >1.0 represent a –A route distortion. The data points suggest an *inverse* correlation, in which none lies exactly on the +A (+60%) \rightarrow RTB \rightarrow –A (70%) route. Data point **1** has a near RTB stereochemistry ($\tau_A = 0.89$), with four data points, **2**–**5**, distorting towards RSBP and having τ_A values in the range 0.75–0.53, best described as SBPDTB stereochemistries. The remaining two data points, **6** and **7**, have τ_A values >1.0 , at 1.32 and 1.26 respectively, suggesting extreme –A route ('seesaw') distorted trigonal bipyramidal stereochemistries,¹ SSDTB. There are no data points on the *inverse* linear correlation from RTB to RSBP, but three data points, **1**, **4** and **6**, lie nearby, with **5** and **7** further removed. Data points **2** and **3** lie off the RTB \rightarrow RSBP trend, due to their slightly long Cu–O distances, which are ≈ 0.1 \AA greater than expected, Table 3.

The Cu–O distances in Fig. 4(b) increase from 1.982(5) to 2.245(4) \AA , while the Cu–N(2,4) distances decrease from 2.094(4) to 2.013(9) \AA , and show a general *inverse* trend. The main –A \rightarrow RTB \rightarrow +A correlation has no data points on it, but there are two data points, **1** and **4**, lying close by. This linear correlation makes an angle of 63.5° with the horizontal and has a slope of *ca.* 2, consistent with the $\Delta\text{Cu–O} = 2\Delta\text{Cu–N(2,4)}$ relationship applying for data points **1** and **4**. The other five data points, **2** and **3**, above, and **5**–**7**, below, lie well off the main correlation. The data points **2** and **3** lie significantly off the main –A \rightarrow RTB \rightarrow +A correlation due to their slightly longer Cu–O distances. The sums of the distances for the two data points, **1** and **4**, which lie almost on the main –A \rightarrow RTB \rightarrow +A correlation are very close to the RTB sum, Table 3.

The data points in Fig. 4(c) show the α_3 values increasing from 99.8(1) to 139.6(1) $^\circ$, $\Delta\alpha_3 = 39.8^\circ$, as the Cu–O distances increase from 1.982(5) to 2.245(4) \AA , $\Delta\text{Cu–O} = 0.263$ \AA , displaying a *normal* trend. There is one data point **1** at near RTB, showing a slight +A route distortion. Four data points, **2**–**5**, have α_3 values $>120^\circ$ and Cu–O values >2.064 \AA , showing +A route distortion. Two data points, **6** and **7**, have α_3 values $<120^\circ$ and Cu–O values <2.064 \AA , showing –A route distortion. The –A \rightarrow RTB \rightarrow +A pathway corresponds to a *normal* correlation, with three data points **1**, **6** and **7** lying very close to the line, **1** on the RTB \rightarrow +A section and **6** and **7** on the RTB \rightarrow –A section. Data points **2** and **3** lie well off the –A \rightarrow RTB \rightarrow +A pathway, with Cu–O distances significantly longer, ≈ 0.1 \AA , than predicted from their α_3 values, while data points **4** and **5** also seem to have slightly longer Cu–O distances, 0.04 \AA , than expected from their corresponding α_3 values. There are two possible lower parallel trend lines involving one data point **4**, with **5** lying nearby, and two data points, **2** and **3**. These linear correlations do not have enough data points to be convincing. However it is significant that the three correlations involve approximately equal separations between the

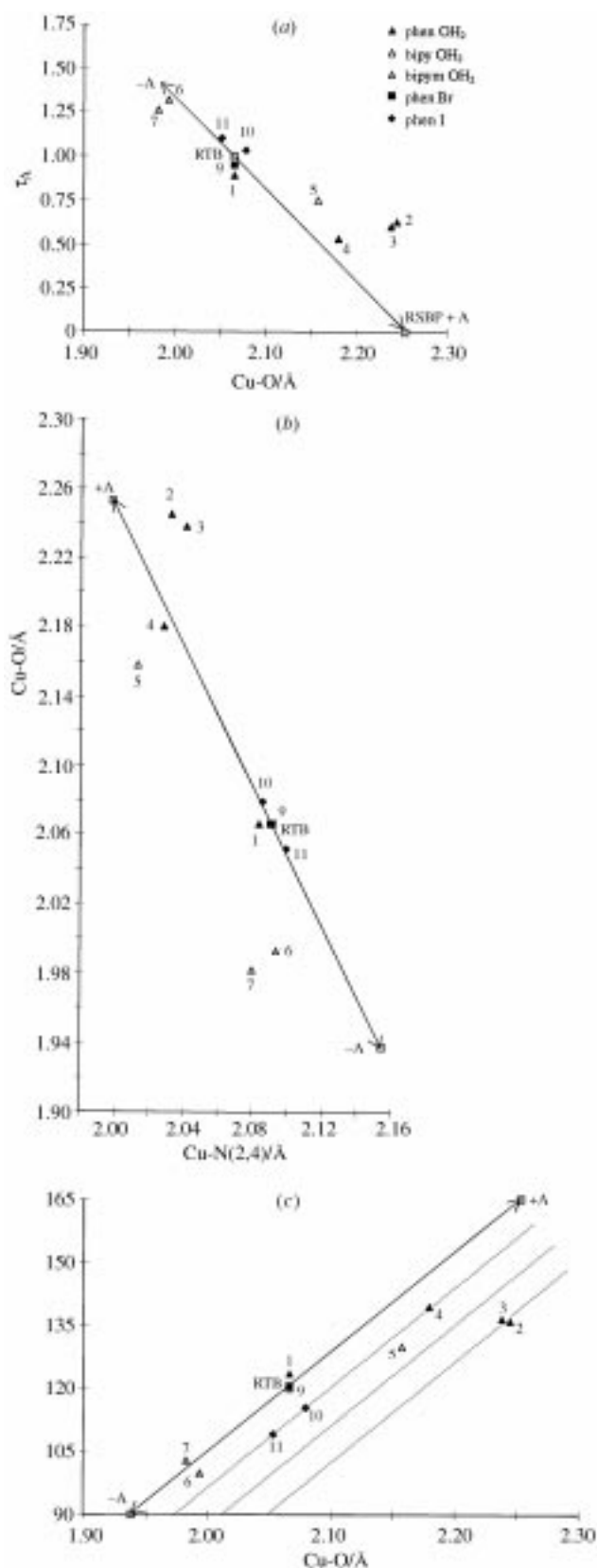


Fig. 4 Scatter plots for the $[\text{Cu}(\text{chelate ligand})_2(\text{OH}_2)][\text{Y}]_2$ complexes

lines of either $\approx 9^\circ$ in the α_3 values or of $\approx 0.035 \text{ \AA}$ in the Cu–O distances.

In general the seven $[\text{Cu}(\text{chelate ligand})_2(\text{OH}_2)][\text{Y}]_2$ data points are hardly sufficient to stand alone in scatter-plot analysis, Fig. 4(a)–4(c), especially as only the four $[\text{Cu}(\text{phen})_2(\text{OH}_2)][\text{Y}]_2$ complexes are strictly cation distortion isomers,²⁸ yet the seven data points show similar trends to those observed previously.¹

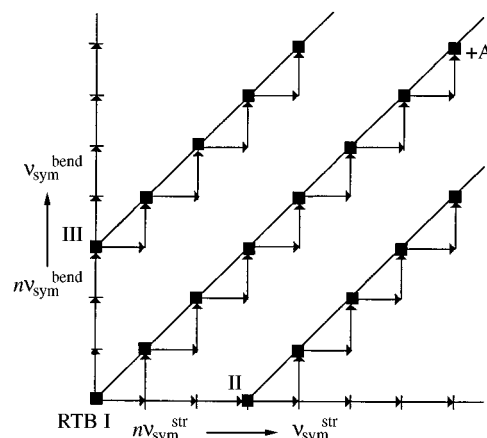


Fig. 5 Diagram illustrating how the linear and parallel correlations are formed by the sequential operation of the $v_{\text{sym}}^{\text{str}}$ and $v_{\text{sym}}^{\text{bend}}$ modes of vibration

Comparison of the $[\text{Cu}(\text{chelate ligand})_2(\text{OH}_2)][\text{Y}]_2$ complexes with other $\pm A$ distorted $[\text{Cu}(\text{chelate})_2\text{X}][\text{Y}]$ complexes

There are seven $[\text{Cu}(\text{chelate ligand})_2(\text{OH}_2)][\text{Y}]_2$ complexes having CuN_4O chromophores and a crystallographic two-fold axis. Since this is quite a limited data set, three other related $\pm A$ route distorted $[\text{Cu}(\text{chelate ligand})_2\text{X}][\text{Y}]$ complexes, where $\text{X} = \text{Br}^-$ or I^- , involving a two-fold axis will be considered. Selected bond lengths and angles are shown in Table 2, with the Cu–X distances, where $\text{X} = \text{Br}^-$ and I^- , corrected to give the equivalent Cu–O distances^{6,7} and added to Fig. 4(a)–4(c) for comparison.

The $[\text{Cu}(\text{phen})_2\text{Br}][\text{ClO}_4]$ complex **9**²⁹ is the nearest experimental data point to a RTB stereochemistry. It has a crystallographic two-fold axis and shows a slight $+A$ route distortion. There are two $[\text{Cu}(\text{phen})_2\text{I}][\text{Y}]$ complexes, **10**³⁰ and **11**,³¹ with a crystallographic two-fold axis and α_3 values $< 120^\circ$, showing a $-A$ route distortion. The three data points **9**–**11** are added to Fig. 4(a)–4(c) to show how close they cluster to the RTB data point. They consolidate the $-A \rightarrow \text{RTB} \rightarrow +A$ route, but do not extend the range of the 60% $+A$ and 70% $-A$ route distortions. However, **10** and **11** do suggest a parallel pathway in Fig. 4(c).

Possible interpretation of the $\pm A$ route distortions in terms of modes of vibration

The extensive range of the Cu–L distances and of the α_n angles for the $[\text{Cu}(\text{phen})_2(\text{OH}_2)][\text{Y}]_2$ complexes, 0.17 \AA and 16° , respectively, Table 2, have only been interpreted in terms of the $\pm A$ route distortions. However, it has been suggested earlier^{1,4,5} that this route due to the crystallographic two-fold axis may be understood, alternatively, in terms of the $v_{\text{sym}}^{\text{str}}$ and $v_{\text{sym}}^{\text{bend}}$ modes of vibration of the CuN_4O chromophore alone, Fig. 1, this notwithstanding the relative magnitudes of the structural changes,³² requiring the ‘amplification factor’³³ of the pseudo-Jahn–Teller effect,³⁴ with a slightly different notation to that given earlier.³⁵

One of the most significant features of Fig. 4(c) is that two of the data points **1** and **7**, three if the data point for **9** is included, lie strictly along the $-A \rightarrow \text{RTB} \rightarrow +A$ pathway, suggesting that the changes in the α_3 angle and Cu–O distance are closely linked. One such linking process suggests that the changes in these parameters are determined only by the underlying nuclear modes of vibration,¹ Fig. 1, suggesting a vibronic coupling mechanism.³⁵ A feature of the parameters of Fig. 4(c) is that the α_3 angle can only be changed by the $v_{\text{sym}}^{\text{bend}}$ mode of vibration and the Cu–O distance can only be changed by the $v_{\text{sym}}^{\text{str}}$ mode of vibration. If such modes operated separately from the RTB (point I), Fig. 5, the former would only produce a vertical linear correlation of data points and the latter a hori-

zonal correlation. While such limited correlations can be identified in Fig. 4(c), the most convincing correlation of two, or three, data points, occurs at an angle of 34° to the Cu–O axis. The only way such a positive correlation can occur is if the two modes of vibration are strongly coupled (they both transform as the A_1 representation in C_{2v} symmetry or as the A representation in C_2 symmetry), as shown in Fig. 5, to produce a stepped displacement. However, such a single displacement due to one quantum of each mode of vibration would still be too small to be observed³² on the scale of Fig. 4(c), namely, 0.005 Å and 1°. For the scale of the $-A \rightarrow \text{RTB} \rightarrow +A$ pathway in Fig. 4(c) to be observed, namely a change of 0.17 Å in the Cu–O distance and a change of 16° in the α_3 angle, a progression of 15–35 coupled vibrations must occur. Such a progression can be considered as a plot of the structural pathway from the $-A$ route to the $+A$ route of Fig. 5, involving the coupled ($v_{\text{sym}}^{\text{str}} + v_{\text{sym}}^{\text{bend}}$) modes of vibration, with the two or three data points representing two or three separate individual steps along the structural pathway, and each data point characterised by full single-crystal structure determination.

In order to explain the occurrence of the parallel correlations in Fig. 4(c), n modes of a **single** vibration, $\pm v$, where $n = 8\text{--}10$, must be involved in order that the parallel displacement can be observed, Fig. 5, points **II** and **III**. This is then followed by a progression of the coupled modes, in order that a linear correlation can be observed, separate but parallel to the central linear correlation. This observation of linear and parallel correlations in the same plot, Fig. 4(c), is one of the best pieces of evidence for both structural pathways and parallel pathways and originates from the ‘amplification factor’³³ in the pseudo-Jahn–Teller Effect.³⁴

The various plots of Fig. 4(a)–4(c) strongly suggest that the directions of distortion from $-A \rightarrow \text{RTB} \rightarrow +A$ route distortion can be associated with the modes of vibration of the CuN_4O chromophore, Fig. 1. The $\pm A$ route is restricted to the $v_{\text{sym}}^{\text{str}}$ and $v_{\text{sym}}^{\text{bend}}$ modes of vibration of C_2 symmetry, with no contribution from the $v_{\text{asym}}^{\text{str}}$ and $v_{\text{asym}}^{\text{bend}}$ modes of vibration. Only when the crystallographic two-fold axis is absent, i.e. C_1 symmetry, all four modes of vibration (A) can contribute as in structure **8**, Table 2. In this respect the $[\text{Cu}(\text{phen})_2(\text{OH}_2)][\text{Y}]_2$ complexes, $\pm A$ route, are different from the lower symmetry $[\text{Cu}(\text{phen})_2\text{Cl}][\text{Y}]$ complexes,¹ $-A + B$ route distortions.

Application to other $\pm A$ distorted five-co-ordinate complexes

While five-co-ordinate copper(II) complexes involving a crystallographic two-fold axis are not common, five other complexes are known, Fig. 6. The complex $[\text{Cu}(\text{py})_3(\text{O}_2\text{NO})_2]$ **12**³⁶ (py = pyridine) has an α_3 angle of 91.4(3)°, in-plane Cu–O(2,4) distances of 2.154(7) Å and a Cu–N distance of 2.064(9) Å, showing an extreme ‘seesaw’ stereochemistry ($-A$), although two additional long Cu–O distances, 2.732(9) Å, suggest it might be described as seven-co-ordinate. Two related but clearly five-co-ordinate structures, $[\text{Cu}(\text{terpy})(\text{NCS})_2]$ **13**³⁷ and $[\text{Cu}(\text{terpy})\text{Br}_2]$ **14**³⁷ (terpy = 2,2'; 6',2''-terpyridine) have higher α_3 angles <120° at 98.1(3) and 109.0(0)°, respectively, which show a smaller $-A$ route distortion and which have been described as a ‘reversed’ trigonal bipyramid.³⁷ A recently reported complex, $[\text{Cu}(\text{hfacac})_2(\text{NH}_3)]$ **15**³⁸ (hfacac = 1,1,1,5,5,5-hexafluoroacetylacetonate) has an α_3 angle of 90.8(2)°, $\alpha_{1,2} = 134.6(1)^\circ$, in-plane Cu–O(2,4) distances of 2.075(3) Å and a short Cu–N distance of 1.933(6) Å, again suggesting an extreme ‘seesaw’ stereochemistry. A related complex, $[\text{Cu}(\text{hfacac})_2(\text{OH}_2)]$ **16**³⁹ with $\alpha_3 = 167.0(1)^\circ$, $\alpha_{1,2} = 96.5(1)^\circ$, short in-plane Cu–O(2,4) distances of 1.94 Å and a long Cu–O distance of 2.204(3) Å, has an extreme $+A$ route distortion, with an approximate RSBP stereochemistry, but still retaining the crystallographic two-fold axis. These two $[\text{Cu}(\text{hfacac})_2\text{X}]$ structures are significant since they display the extreme stereochemistries of the ‘seesaw’ structure ($-A$ route), **15**, and RSBP ($+A$ route), **16**, involving a difference in the α_3 angle of 76.2°. Together, these five

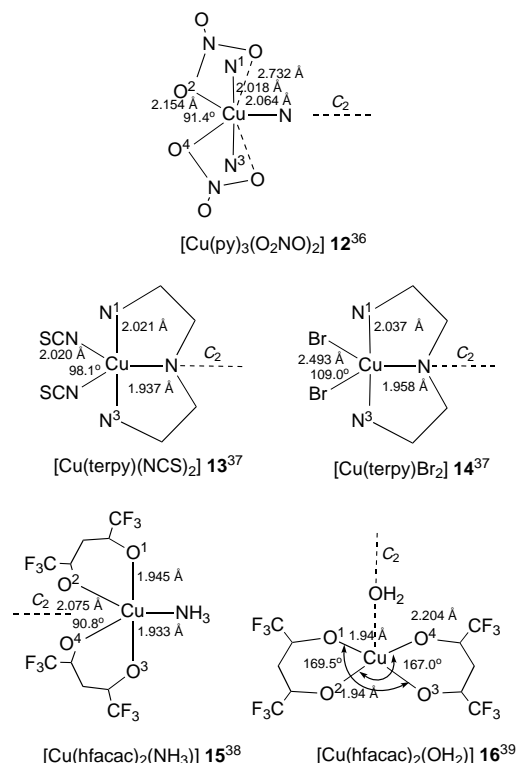


Fig. 6 Molecular structures of some $\pm A$ route distorted complexes

additional copper(II) complexes clearly demonstrate the range of the $\pm A$ route distortion and the associated crystallographic two-fold axis. However, while the RSBP stereochemistry of the $+A$ route has been known for some time, the recognition of the extreme $-A$ route ‘seesaw’ stereochemistry has only recently been recognised.¹ From this series of $\pm A$ route $[\text{Cu}(\text{chelate ligand})_2\text{X}][\text{Y}]$ complexes there is no obvious connection between these $\pm A$ route structures and the identity of X; equally there is no apparent reason why the $\text{X} = \text{Cl}^-$ complexes are dominated by a $-A + B$ route distortion.¹

Electronic properties of the $[\text{Cu}(\text{phen})_2(\text{OH}_2)][\text{Y}]_2$ complexes

The polycrystalline electronic reflectance spectra of complexes **1**, **2** and **4** show broad asymmetric peaks at 11 700, 12 700 and 12 400 cm^{-1} respectively, with possible high-energy shoulders at 14 700, 15 200 and 15 100 cm^{-1} . The spectrum for **1** is consistent with a near RTB stereochemistry,^{40,41} showing a slight distortion towards SBP. For **2** and **4** the spectra suggest an increased SBP distortion, relative to **1**, indicated by the movement of the peaks to higher energy. The one-electron ground-state configuration⁴⁰ is $d_{xz} > d_{xy} \approx d_{x^2-y^2} > d_{zx} \approx d_{yz}$. The principal absorption may be assigned as a $d_{x^2-y^2} \rightarrow d_{xz}$ transition, with the high-energy shoulder assigned as a $d_{xz} \approx d_{yz} \rightarrow d_{xz}$ transition. The electronic spectra reflect the distortion of the stereochemistries from RTB. A RTB stereochemistry is characterised by a broad asymmetric peak at $\approx 11\,500\text{ cm}^{-1}$, with a possible high-energy shoulder at $\approx 14\,500\text{ cm}^{-1}$. The peaks move to higher energy as the extent of SBP distortion increases, as seen for **2** which has a broad peak at 12 700 cm^{-1} and a possible high-energy shoulder at 15 200 cm^{-1} .

The ESR spectra⁴⁰ of complexes **3–5**, Table 5 and Fig. 7(a), suggest an axially compressed CuN_4O chromophore stereochemistry with $g_3 \approx g_2 \gg g_1 \approx 2.0$, and are consistent with an approximately d_{xz} ground state.^{40,41} This is compatible with the distorted trigonal bipyramidal copper(II) stereochemistry for all four complexes. The electronic spectra of complexes **3–5**, Fig. 7(b), involve a single intense peak at $\text{ca. } 12\,500\text{ cm}^{-1}$, with some evidence for a weak shoulder on the high-energy side, again consistent with the basic trigonal bipyramidal stereochemistry.⁴⁰

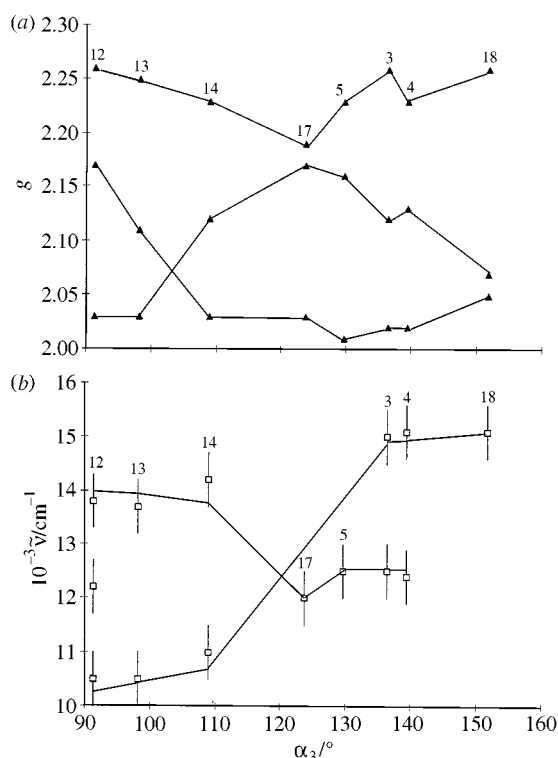


Fig. 7 Plots of electronic properties (g values and energy) versus the α_3 angle

Table 5 The g values and electronic energies for selected $\pm A$ distorted complexes

Complex	$\alpha_3/^\circ$	g	$\tilde{\nu}/\text{cm}^{-1}$
12 $[\text{Cu}(\text{py})_3(\text{O}_2\text{NO})_2]^{36}$	91.4	2.03	10 500
		2.17	12 200
		2.26	13 800
13 $[\text{Cu}(\text{terpy})(\text{NCS})_2]^{37}$	98.1	2.03	10 500
		2.11	13 700
		2.25	
14 $[\text{Cu}(\text{terpy})\text{Br}_2]^{37}$	109.0	2.03	11 000
		2.12	14 200
		2.23	
17 $[\text{Cu}(\text{bipy})_2\text{Cl}][\text{PF}_6]\cdot\text{H}_2\text{O}^{42}$	123.8	2.03	12 000
		2.17	
		2.19	
5 $[\text{Cu}(\text{bipy})_2(\text{OH}_2)][\text{S}_2\text{O}_8]^{24}$	129.8	2.01	12 500
		2.16	
		2.23	
3 $[\text{Cu}(\text{phen})_2(\text{OH}_2)][\text{BF}_4]^{12,24}$	136.6	2.02	12 500
		2.12	15 000
		2.26	
4 $[\text{Cu}(\text{phen})_2(\text{OH}_2)][\text{NO}_3]^{13,24}$	139.6	2.02	12 400
		2.13	15 100
		2.23	
18 $[\text{Cu}(\text{bipy})_2(\text{O}_2\text{ClO}_2)][\text{ClO}_4]^{43}$	151.8	2.05	15 100
		2.07	
		2.26	

Structural pathways and electronic properties

The structural pathway of Fig. 1 offers one of the most extensive pathways for a structurally related series of copper(II) complexes.^{3,41} If the appropriate g values and electronic energies of the complexes, Table 5, are plotted against their α_3 values, the ESR g values vary as shown in Fig. 7(a) and the electronic energies as in Fig. 7(b). There is clearly a systematic variation of the g values over an α_3 range of 60° . The variation in the average electronic energies is less convincing, but together they highlight the value of the structural pathway of Fig. 1 in correlating^{2,41} the electronic properties of comparable copper(II) complexes⁴⁴ along a structural pathway. Such pathways may then be applied

in two ways, (a) to predict the electronic properties of corresponding complexes of known crystal structure,⁴⁴ and (b) to predict the structure of related complexes from a knowledge of their electronic properties, such as under pressure⁴⁵ or after heating.⁴⁶

Acknowledgements

The authors acknowledge the award of Forbairt grants and U.C.C. Studentships (to G. M., C. M. and B. M.), the Irish Science and Technology Agency (EOLAS) and U.C.C. for capital grants for the purchase of the CAD4 X-ray diffractometer, U.C.C. for a capital grant for a Shimadzu UV-VIS-NIR 3101 PC spectrometer, the Computer Bureau, U.C.C., for computing facilities, Professor G. M. Sheldrick, Drs. P. Roberts, K. Henrick, P. McCardle and A. L. Spek for the use of their programs and the Microanalysis Section, U.C.C., for analysis.

References

- Part 3, G. Murphy, P. Nagle, B. Murphy and B. J. Hathaway, preceding paper.
- H. Burgi and J. D. Dunitz, *Acc. Chem. Res.*, 1983, **16**, 153; J. D. Dunitz, *X-Ray Analysis and Structure of Organic Molecules*, Cornell University Press, London, 1979, ch. 7.
- B. J. Hathaway, *Struct. Bonding (Berlin)*, 1984, **57**, 55.
- W. D. Harrison, D. M. Kennedy, N. J. Ray, R. Sheahan and B. J. Hathaway, *J. Chem. Soc., Dalton Trans.*, 1981, 1556.
- P. Nagle, E. O'Sullivan, B. J. Hathaway and E. Muller, *J. Chem. Soc., Dalton Trans.*, 1990, 3399.
- E. Muller, C. Piguet, G. Berardinelli and A. F. Williams, *Inorg. Chem.*, 1988, **27**, 849.
- E. Muller, FACAN, program for factor analysis, written in Turbo Pascal (IBM and compatible), 1989.
- E. R. Malinowski and D. G. Howery, *Factor Analysis in Chemistry*, Wiley, New York, 1980.
- D. Cunningham, Ph.D. Thesis, National University of Ireland, 1992.
- A. W. Addison, T. Nageswara Rao, J. Reedijk, J. van Rijn and G. C. Verschoor, *J. Chem. Soc., Dalton Trans.*, 1984, 1349.
- M. Liu and S. K. Arora, *Acta Crystallogr., Sect. C*, 1993, **49**, 373.
- H. Nakai and Y. Deguchi, *Bull. Chem. Soc. Jpn.*, 1975, **48**, 2557.
- H. Nakai and Y. Noda, *Bull. Chem. Soc. Jpn.*, 1978, **51**, 1386.
- P. McCardle, XCAD, program for data reduction of CAD4 output, University College Galway, 1990.
- G. M. Sheldrick, SHELX 76, program for X-ray crystal structure determination, University of Cambridge, 1976.
- G. M. Sheldrick, SHELXS 86, program for X-ray crystal structure solution, University of Göttingen, 1986.
- D. T. Cromer and J. T. Waber, *International Tables for X-Ray Crystallography*, Kynoch Press, Birmingham, 1974, vol. 4, pp. 71, 148 (Present distributor, Kluwer, Dordrecht).
- P. Roberts and G. M. Sheldrick, XANADU, program for the calculation of crystallographic data, University of Cambridge, 1979.
- K. Henrick, PUBTAB, program to prepare and print crystallographic tables for publication, Polytechnic of North London, 1980.
- A. L. Spek, PLUTON 92, graphics program to prepare and print molecular structures, University of Utrecht, 1992.
- F. Huq and A. C. Shapski, *J. Chem. Soc. A*, 1971, 1927.
- R. J. Fereday, P. Hodgson, S. Tyagi and B. J. Hathaway, *J. Chem. Soc., Dalton Trans.*, 1981, 2070.
- W. D. Harrison and B. J. Hathaway, *Acta Crystallogr., Sect. B*, 1980, **36**, 1069.
- W. D. Harrison and B. J. Hathaway, *Acta Crystallogr., Sect. B*, 1979, **35**, 2910.
- L. W. Morgan, W. T. Pennington, J. D. Petersen, R. R. Ruminski, D. W. Bennett and J. S. Rommel, *Acta Crystallogr., Sect. C*, 1992, **48**, 163.
- G. De Munno, G. Bruno, M. Julve and M. Romeo, *Acta Crystallogr., Sect. C*, 1990, **46**, 1828.
- W. D. Harrison, B. J. Hathaway and D. Kennedy, *Acta Crystallogr., Sect. B*, 1979, **35**, 2301.
- N. Ray, L. Hulett, R. Sheahan and B. J. Hathaway, *J. Chem. Soc., Dalton Trans.*, 1981, 1463.
- O. J. Parker, G. T. Greiner, G. L. Breneman and R. D. Willett, *Polyhedron*, 1994, **2**, 267.
- C. Harrington and B. J. Hathaway, unpublished work.
- T. W. Hambley, C. L. Raston and A. H. White, *Aust. J. Chem.*, 1977, **30**, 1965.

- 32 P. Brint, personal communication.
- 33 I. B. Bersuker, *Coord. Chem. Rev.*, 1975, **14**, 357.
- 34 I. B. Bersuker, *The Jahn–Teller Effect and Vibronic Interactions in Modern Chemistry*, Plenum, New York, 1983.
- 35 D. Reinen, *Comments Inorg. Chem.*, 1983, **2**, 227; D. Reinen and M. Atanasov, *J. Chem. Phys.*, 1989, **136**, 27; *Magn. Reson. Rev.* 1991, **15**, 167.
- 36 A. F. Cameron, D. W. Taylor and R. H. Nuttall, *J. Chem. Soc., Dalton Trans.*, 1972, 1603; R. J. Dudley, B. J. Hathaway, P. G. Hodgson, P. C. Power and D. J. Loose, *J. Chem. Soc., Dalton Trans.*, 1974, 1005.
- 37 M. J. Arriortua, J. L. Mesa, T. Rojo, T. Debaerdemaeker, D. Beltran-Porter, H. Stratemeier and D. Reinen, *Inorg. Chem.*, 1988, **27**, 2976.
- 38 J. Pinkas, J. C. Huffman, M. H. Chisholm and K. G. Caulton, *Inorg. Chem.*, 1995, **34**, 5314.
- 39 L. Funk and T. R. Ortolano, *Inorg. Chem.*, 1968, **7**, 567; J. Pinkas, J. C. Huffman, D. V. Baxter and M. H. Chisholm, *Chem. Mater.*, 1995, **7**, 1589.
- 40 B. J. Hathaway and D. E. Billing, *Coord. Chem. Rev.*, 1970, **5**, 143.
- 41 B. J. Hathaway, *Comprehensive Coordination Chemistry. The Synthesis, Reactions, Properties and Applications of Coordination Compounds*, eds. G. Wilkinson, R. D. Gillard and J. A. McCleverty, Pergamon, Oxford, 1988, vol. 5, pp. 533–774.
- 42 S. Tyagi, B. J. Hathaway, S. Kremer, H. Stratemeier and D. Reinen, *J. Chem. Soc., Dalton Trans.*, 1984, 2087.
- 43 J. Foley, D. Kennefick, S. Tyagi and B. J. Hathaway, *J. Chem. Soc., Dalton Trans.*, 1983, 2333; H. Nakai, *Bull. Chem. Soc. Jpn.*, 1971, **44**, 2412.
- 44 B. J. Hathaway, *J. Chem. Soc., Dalton Trans.*, 1972, 1196.
- 45 K. L. Bray and H. G. Drickamer, *J. Phys. Chem.*, 1989, **93**, 7604; H. C. Drickamer and K. L. Bray, *Acc. Chem. Res.*, 1990, **23**, 55.
- 46 A. A. G. Tomlinson and B. J. Hathaway, *Coord. Chem.*, 1970, **5**, 1.

Received 26th March 1997; Paper 7/02293J